Journal Pre-proof

Cleavage of FNDC5 and insights into its maturation process

Yongwei Nie, Bai Dai, Xudong Guo, Dongjun Liu

PII: S0303-7207(20)30140-4

DOI: https://doi.org/10.1016/j.mce.2020.110840

Reference: MCE 110840

To appear in: *Molecular and Cellular Endocrinology*

Received Date: 8 January 2020

Revised Date: 20 April 2020

Accepted Date: 23 April 2020

Please cite this article as: Nie, Y., Dai, B., Guo, X., Liu, D., Cleavage of FNDC5 and insights into its maturation process, *Molecular and Cellular Endocrinology* (2020), doi: https://doi.org/10.1016/j.mce.2020.110840.

CRediT author statement

Dongjun Liu and **Xudong Guo**: Supervision. **Yongwei Nie**: Conceptualization, Methodology, Investigation, Data curation, Writing-Original draft preparation. **Bai Dai**: Software, Visualization. All authors have read and approved the final manuscript.

Cleavage of FNDC5 and insights into its maturation process

Yongwei Nie [1, 2], Bai Dai [1], Xudong Guo [1, *] and Dongjun Liu [1, *]

From the [1]State Key Laboratory of Reproductive Regulation & Breeding of Grassland Livestock, Inner Mongolia University, Hohhot, China; [2]School of Medicine, Nankai University, 94 Weijin Road, Tianjin 300071, China

***** To whom correspondence should be addressed:
Xudong Guo: State Key Laboratory of Reproductive Regulation & Breeding of Grassland Livestock, Inner Mongolia University, Hohhot, China; bixdguo@imu.edu.cn; Dongjun Liu: State Key Laboratory of Reproductive Regulation & Breeding of Grassland Livestock, Inner Mongolia University, Hohhot, China; nmliudongjun@sina.com

Keywords: FNDC5; cleavage; maturation; peptides; glycation
(Word count: 24694; tables: 0; figures: 5; references: 29; supporting information: 1)

Abstract

FNDC5 corresponds to an irisin precursor that increases with exercise. Studies suggest that irisin mediates beneficial effects in adipose tissues, skeletal muscle, bone, and brain. However, the cleavage and maturation processes of FNDC5 have not been clearly identified. This study aimed to show that the signal peptide and transmembrane domain of FNDC5 were associated with the secretion of its ectodomain. Localization studies identified the signal peptide that was responsible for endoplasmic reticulum targeting activity of nascent FNDC5 and showed that the FNDC5 ectodomain corresponding to irisin could be transported across the membrane by a transmembrane domain. Analysis of cleavage constructs revealed that the ectodomain of FNDC5 could be cleaved from its signal peptide and transmembrane attachment. Genetic ablation of the signal peptide cleavage site blocked N-glycosylation of FNDC5. Identification of the FNDC5 maturation process should facilitate our understanding of irisin secretion.

Introduction

FNDC5 (fibronectin domain-containing protein 5) was initially discovered and characterized by two research groups with a focus on the fibronectin type III repeat domain and the peroxisomal targeting motif, respectively (Ferrer-Martinez et al., 2002; Teufel et al., 2002). In examining the metabolic benefits of exercise that are expressed by muscle in response to PGC-1α activation, irisin has been identified as a myokine that is produced after cleavage of the ectodomain portion of the type I membrane protein, FNDC5 (Bostrom et al., 2012).

Following the initial description of irisin, many authors have tried to identify its physiological role. Studies suggest that irisin mediates certain beneficial effects in adipose tissues, skeletal muscle, bone, and brain (Colaianni et al., 2015; Reza et al., 2017; Wrann et al., 2013; Xiong et al., 2018). In particular, irisin has been shown to mediate the thermogenesis of white adipose tissue (Bostrom et al., 2012; Zhang et al., 2014). Since the peptide was first described, interest in its therapeutic potential has increased and been linked to a wide range of therapeutic effects, including improved metabolism, energy homeostasis, cardiovascular health, and cognition (Leal et al., 2018; Young et al., 2019).

The reported circulating concentrations of irisin seem to differ dramatically in human serum or plasma, which have raised doubts about the validity of the commercial enzyme-linked immunosorbent assay (ELISA) kits used to detect circulating irisin and even about the existence of irisin in humans (Crujeiras et al., 2015; Polyzos et al., 2015). Undervaluation data obtained from tandem mass spectrometry reveal that irisin circulates at a level at or above the levels quantitated for many other important biological hormones, such as leptin and insulin (Jedrychowski et al., 2015). These findings confirm the actual existence of irisin in humans. Information regarding different FNDC5 protein fragments, the presence of mature or precursor forms of irisin, and glycosylation of the protein probably contribute to immunoassay quality and irisin detection accuracy (Erickson, 2013; Perakakis et al., 2017).

The irisin sequence was described in 2012 by Bostrom et al. Using mass spectrometry, the irisin peptide (KDEVTMKE) was found in the medium of the N-terminus of FNDC5 (without the signal peptide) fused with the C-terminus of the FC-domain of IgG construct (Bostrom et al., 2012). The peptide sequence was consistent with amino acids 133-140 of FNDC5 according to UniProt entry Q8K4Z2. The peptide that was shed into the media might have been only a small portion of the irisin. The protein could be detected in serum, but cleavage site(s) and exact size both remain a matter of debate (Sanchis-Gomar et al., 2015). Therefore, the formation sequence of the irisin precursor is needed to better understand how secreted irisin is formed. In addition, validating whether irisin is actively cleaved from FNDC5 might explain the differences in circulating concentrations of irisin between acute and chronic training and reveal additional stimulators of irisin secretion. The data obtained in this study identify the cleavage and maturation process of FNDC5 by fusing different FNDC5 protein fragments with DsRed2 and/or EGFP and should facilitate an improved detection of irisin in physiological concentrations.

Materials and Methods

Bioinformatic identification of FNDC5

The signal peptide sequence of FNDC5 was analyzed using SignalP-software (http://www.cbs.dtu.dk/services/SignalP/) (Petersen et al., 2011). Sequences with positive C, Y, S, and D-scores were considered positive for a signal sequence. The transmembrane domain of FNDC5 was analyzed in the Phobius web interface (http://phobius.cgb.ki.se) (Kall et al., 2004). Phobius provides a list of the location of the predicted transmembrane helices. If the whole sequence is labeled as cytoplasmic or non-cytoplasmic, the prediction is that it contains no membrane helices.

Plasmid construction

To express FNDC5 and its different domains as EGFP or DsRed2 tagged fusion proteins, the DNA sequences coding FNDC5 and its different domains were cloned into pEGFP-C1, pEGFP-N1, or pDsRed2-C1 vectors (Clontech, USA), respectively, to produce the following: N-terminus of FNDC5 fused with EGFP (pEGFP-C1-FNDC5); C-terminus of FNDC5 fused with EGFP (pEGFP-N1-FNDC5); N-terminus of signal peptide fused with EGFP (pEGFP-C1-SP); N-terminus of signal peptide fused with DsRed2 (pDsRed2-C1-SP); N-terminus of transmembrane-cytoplasmic (C) domains fused with EGFP (pEGFP-C1-TM-C); and N-terminus of irisin-transmembrane-cytoplasmic domains fused with EGFP (pEGFP-C1-irisin-TM-C). To analyze FNDC5 cleavage, a plasmid called pDsRed2-C1-FNDC5-EGFP-N1 was constructed. Potential ectodomain-cleavage-deficient mutants (pEGFP-N1-FNDC5deletion^{139}KE^{140}) were constructed via site-directed mutagenesis of pEGFP-N1-FNDC5 using the QuikChange strategy with high-fidelity Pfu DNA polymerase (TaKaRa, China) and verified by sequencing. Signal-peptide-cleavage-deficient mutants (pEGFP-N1-FNDC5 deletion^{28}AD^{29}), N-terminus of irisin fused with EGFP (pEGFP-C1-Irisin), and N-terminus of transmembrane domains (TM) fused with EGFP (pEGFP-C1-TM) have been previously described (Nie and Liu, 2017). pDsRed2-C1-EGFP-N1 and pDsRed2-C1-NLS-EGFP-N1 were constructed as EGFP and DsRed2 fusion control plasmids.

Cell transfection and fluorescence microscopy

Human HeLa and 293T cells were cultured in DMEM medium (Gibco, USA) supplemented with 10% fetal calf serum, 100 U of penicillin, and 100 μg/mL streptomycin. Cells were grown at 37°C in a humidifier with a 5% CO_2 atmosphere. Cells were transfected with the indicated plasmids using Lipofectamine™ 2000 transfection reagent (Thermo Fisher Scientific, USA) according to the manufacturer's protocol. The fluorescent pattern was viewed using a Nikon AIR laser-scanning confocal microscope.

Antibodies and reagents

The following antibodies and reagents were used: EGFP (sc-8334, Santa Cruz Biotechnology, 1:1000, v/v), irisin (ab174833, Abcam, 1:1000, v/v), α-tubulin (ab15246, Abcam, 1:100, v/v), FITC labeled goat anti-rabbit IgG (ab6717, Abcam, 1:1000, v/v), HRP labeled goat anti-rabbit IgG (ab6721, Abcam, 1:10000, v/v), PNGase F (P0704S, New England Biolabs), RIPA Lysis Buffer (20-188, Millipore), Protease Inhibitor Cocktail (P8340, Sigma-Aldrich), TBST buffer (CW0043, Cwbiotech, China), BCA Protein Assay Kit (23225, Thermo Fisher Scientific), ECL Plus Western Blotting Substrate (32132, Thermo Fisher Scientific), and Prestained Protein Ladder (26616, Thermo Fisher Scientific).

Western Blotting analysis

Whole cell lysates were prepared by separately adding 1 mL of RIPA Lysis Buffer and 5 μL Protease Inhibitor Cocktail to each of the groups. After a 30-minute incubation on ice, samples were centrifuged at

12,000 rpm for 15 minutes at 4°C to pellet cellular material, and supernatants were assessed for protein concentrations. Protein concentrations were assessed using the BCA Protein Assay Kit according to the manufacturer's protocol. Western blotting was performed as follows: whole cell lysates in RIPA lysis buffer were mixed with 5× SDS-PAGE sample buffer. Proteins were subjected to SDS-PAGE with a 12% acrylamide gel. The gel-separated proteins were transferred to PVDF membranes, incubated with primary antibodies overnight at 4°C, and probed with HRP labeled secondary antibodies for 1 hour at room temperature. The PVDF membranes with protein-antibody complexes were washed three times using TBST buffer. The proteins on the PVDF membranes were visualized with Thermo Scientific Pierce ECL Plus Western Blotting Substrate on a Tanon 5200 (Tanon, China) detection system. The experiment was repeated at least three times.

Results

Identification of potential transport signals within the FNDC5 protein

As shown in Figure 1A, FNDC5 in mice contains 209 amino acids with a 28 amino acid signal peptide N-terminal, followed by an ectodomain domain, a transmembrane domain spanning 152-170 amino acids, and a cytoplasmic domain segment. Using SignalP 4.1 server, we found that FNDC5 contains an N-terminal signal peptide sequence and that the cleavage site is located between ^{28}A and ^{29}D (Figure 1B). Phobius analysis revealed that FNDC5 contained transmembrane helices. The N-terminal sequence of the transmembrane helices was the non-cytoplasmic portion and the C-terminal sequence of the transmembrane helices was the cytoplasmic portion (Figure 1C).

Localization of constructs containing transport signals

Constructs containing transport signals were prepared (Figure 2B) and verified by sequencing and western blotting analysis (Figure 2D) and subcellular localization was evaluated. As shown in Figure 2A, DsRed2 labeled signal peptide (DsRed2-SP fusion protein) was observed in a vesicular-like compartment around the nucleus in FITC labelled α-tubulin HeLa cells. To determine the specific vesicular compartment in which the signal peptide was localized, we co-transfected EGFP labeled signal peptide (EGFP-SP fusion protein) and pDsRed2-ER vector (an ER labeling marker). The co-localization of EGFP-SP with DsRed2-ER indicates that the signal peptide is an ER transport signal. To identify the transmembrane domains responsible for the transmembrane localization of the ectodomain, we constructed combinatorial fragments of FNDC5 domains without a signal peptide. As shown in Figure 2C, EGFP-TM was localized in the cytomembrane. EGFP-irisin-TM-C behaved similarly to EGFP-TM-C with respect to transmembrane localization.

FNDC5 cleavage

We generated non-cleavage cytoplasm localization control by fusing DsRed2 with EGFP, and non-cleavage nucleus localization control by fusing nuclear localization signals (NLS) with DsRed2-EGFP. As shown in Figure 3A, the yellow fluorescence of DsRed2-EGFP was evenly distributed throughout the cytoplasm, and the yellow fluorescence of DsRed2-NLS-EGFP was evenly distributed throughout the cell nucleus in HeLa cells. Exploration of the fluorescent pattern of DsRed2-FNDC5-EGFP showed that the red and green fluorescence were slightly merged (Figure 3B). The red fluorescence of the DsRed2-FNDC5-EGFP protein was observed in a vesicular-like compartment. These results suggested that FNDC5 occurs during proteolytic cleavage.

In view of the proteolytic cleavage of FNDC5, we compared DsRed2-FNDC5-EGFP constructs with constructs containing various transport signals in the lysates of 293T cells by western blotting. In cells transfected with the pDsRed2-C1-FNDC5R-EGFP-N1 plasmid (Figure 3C, lane 5), a 30 kDa cleavage product was observed, which was in agreement with the signal peptide cleavage form (DsRed2-SP) of

DsRed2-FNDC5-EGFP. Meanwhile, we observed a 50 kDa cleavage product (Irisin-TM-C-EGFP), which was similar to the EGFP-Irisin-TM-C construct (Figure 3C, lane 3) and the signal peptide cleavage product of FNDC5-EGFP construct (Figure 3C, lane 6). In addition, a 36 kDa cleavage product (TM-C-EGFP) was observed, which was in agreement with the EGFP-TM-C construct (Figure 3C, lane 2) and the signal peptide and irisin cleaved product of FNDC5-EGFP construct (Figure 3C, lane 6).

Effect of cleavage-deficient mutation on N-glycosylation of FNDC5

To investigate the role of the signal peptide cleavage and transmembrane domain cleavage during FNDC5 maturation, a signal-peptide-cleavage-deficient mutant by alanine and aspartate acid deletion (deletion ^{28}AD^{29}) and a potential ectodomain-cleavage-deficient mutant by lysine and glutamic acid deletion (deletion ^{139}KE^{140}) were forcibly expressed in 293T cells. PNGase F was used to remove the entire N-glycan structure. FNDC5-EGFP (Figure 4A lane 1) and FNDC5-EGFP-deletion^{139}KE^{140} (Figure 4A lane 4) proteins displayed a highly heterogeneous molecular weight pattern. The heterogeneous pattern changed after PNGase F treatment (Figure 4B lanes 1 and 4), and the latter band was in agreement with the predicted molecular weight of FNDC5-EGFP protein. However, EGFP-FNDC5 (Figure 4A lane 2) and FNDC5-EGFP-deletion^{28}AD^{29} (Figure 4A lane 3) proteins displayed little or no glycosylation pattern compared to that of the FNDC5-EGFP protein. Moreover, the pattern was slightly decreased by PNGase F treatment (Figure 4B lanes 2 and 3). Meanwhile, the same result was obtained using anti-FNDC5 antibody detection (Figure 4C and Figure 4D).

Discussion

Irisin is a myokine secreted into circulation by skeletal muscles under certain physiological conditions, such as aerobic training (Figure 5). Furthermore, the localization of irisin sequences alone (EGFP-irisin) has been previously described (Nie and Liu, 2017). We have shown that FNDC5 contains an N-terminal signal sequence (Figure 1B) and that the signal peptide of FNDC5 can result in the retention or retrieval of nascent FNDC5 in the ER (Figure 2A). The signal peptide contains two arginines (11R and 15R) in the middle, and an aromatic amino acid, tryptophan (8W and 17W), at both ends (Figure 1A) that possibly conforms to the arginine-based ER localization consensus motif Φ/Ψ/RRXR (Michelsen et al., 2005; Nie et al., 2016) (where Φ/Ψ denotes an aromatic or bulky hydrophobic residue and X represents any amino acid).

Fluorescence analysis of the cleavage construct (pDsRed2-C1-FNDC5-EGFP-N1) revealed that the signal peptide and transmembrane domain cleavage products were partially merged (Figure 3B). In the lysates of 293T cells transfected with the cleavage construct plasmid, the 30 kDa fragment observed corresponded to the signal peptide cleavage form (DsRed2-SP) of DsRed2-FNDC5-EGFP. In addition, a 53 kDa cleavage product (irisin-TM-C-EGFP) wherein the DsRed2-signal peptide was cleaved was observed (Figure 3C). These results suggested that the presence of the signal peptide maintained ER retention or retrieval of FNDC5 until it was masked as a result of signal sequence cleavage. The findings also suggest that FNDC5 maturation includes at least two proteolytic cleavages: one between the signal peptide and ectodomain, and the other between the ectodomain and transmembrane domain.

Nascent secretory protein synthesis begins in the ER, which is charged with the tasks of correctly integrating nascent proteins and ensuring correct post-translational modification and folding (Barlowe and Miller, 2013; Dancourt and Barlowe, 2010). The removal of the signal peptide cleavage site (deletion ^{28}AD^{29}) has a significant effect on the N-glycosylation of FNDC5, which is mostly retained in the ER [14]. In addition, the removal of a potential ectodomain cleavage site (deletion ^{139}KE^{140}) was observed, similar to that of wild type FNDC5 (Figure 4). The experiments suggested that signal peptide sequence cleavage of nascent FNDC5 occurs before downstream N-glycosylation tasks take place.

Once secretory protein FNDC5 has completed its signal peptide cleavage and N-glycosylation modification, it becomes capable of forward traffic. We have examined the possible contribution of each of the transmembrane containing segments of FNDC5 to ectodomain transmembrane localization, which

was achieved by chimera constructs (EGFP-TM, EGFP-TM-C, and EGFP-irisin-TM-C). The EGFP-irisin-TM-C construct behaves similarly to EGFP-TM-C with respect to transmembrane localization and is independent of irisin sequences (Figure 2C). Therefore, the ability of the FNDC5 transmembrane domain to act as an inserted membrane transport signal is a striking feature.

Crucial data obtained from co-immunoprecipitation study revealed that aV family integrin complexes are irisin receptors in osteocyte (Kim et al., 2019). The findings re-kindled interest in irisin as a candidate target in the treatment of osteoporosis and raised a concern that its use for the browning of adipose tissue, might also lead to osteoporosis (Anastasilakis et al., 2019; Farmer, 2019). Moreover, the research progress of irisin in heart disease, Alzheimer's disease, and dihydromyricetin stimulation of irisin secretion has made encouraging progress (Li et al., 2018; Lourenco et al., 2019; Zhou et al., 2015). Our current data allowed us to clearly identify the cleavage between the signal peptide and ectodomain, and the other between the ectodomain and transmembrane domain. Furthermore, based on the results shown in our Supporting Information, a 35 kDa cleavage fragment (TM-C-EGFP) was observed in lysates of 293T cells transfected with the pEGFP-N1-FNDC5deletion^{139}KE^{140} plasmid. We favor the possibility that the precise proteolytic cleavage site between the ectodomain and transmembrane domain position does not occur merely between ^{140}E and ^{141}M.

In view of the findings reported here, the proteolytic cleavages of FNDC5 are evident. FNDC5 maturation includes at least two proteolytic cleavages: one between the signal peptide and ectodomain, and the other between the ectodomain and transmembrane domain. Our findings provide experimental evidence regarding the functioning of the irisin and FNDC5 with the aspect of cleavage and maturation. Further studies are needed to explore the precise ectodomain cleavage sites and the molecular mechanism of cleavage regulation. Moreover, studies on the mechanisms involved in the proteolytic cleavages would allow us to assess stimulators of irisin secretion.

Acknowledgements: The authors would like to thank Editage for English language editing assistance with the preparation of this article.

Authors' Contribution: Dongjun Liu and Xudong Guo: Supervision. Yongwei Nie: Conceptualization, Methodology, Investigation, Data curation, Writing-Original draft preparation. Bai Dai: Software, Visualization. All authors have read and approved the final manuscript.

Conflicts of Interest: The authors declare that they have no conflicts of interest with the contents of this article.

References

Anastasilakis, A.D., Polyzos, S.A., Makras, P., Douni, E., and Mantzoros, C.S. (2019). Irisin: good or bad for the bone? A new path forward after the reported discovery of irisin receptor? Metabolism - Clinical and Experimental 93, 100-102.

Barlowe, C.K. and Miller, E.A. (2013). Secretory protein biogenesis and traffic in the early secretory pathway. Genetics 193, 383-410.

Bostrom, P., Wu, J., Jedrychowski, M.P., Korde, A., Ye, L., Lo, J.C., Rasbach, K.A., Bostrom, E.A., Choi, J.H., Long, J.Z., et al. (2012). A PGC1-alpha-dependent myokine that drives brown-fat-like development of white fat and thermogenesis. Nature 481, 463-468.

Colaianni, G., Cuscito, C., Mongelli, T., Pignataro, P., Buccoliero, C., Liu, P., Lu, P., Sartini, L., Di Comite, M., Mori, G., et al. (2015). The myokine irisin increases cortical bone mass. Proc Natl Acad Sci U S A 112, 12157-12162.

Crujeiras, A.B., Pardo, M., and Casanueva, F.F. (2015). Irisin: 'fat' or artefact. Clin Endocrinol (Oxf) 82, 467-474.

Dancourt, J. and Barlowe, C. (2010). Protein sorting receptors in the early secretory pathway. Annu Rev Biochem 79, 777-802.

Erickson, H.P. (2013). Irisin and FNDC5 in retrospect: An exercise hormone or a transmembrane receptor? Adipocyte 2, 289-293.

Farmer, S.R. (2019). Boning Up on Irisin. New England Journal of Medicine 380, 1480-1482.

Ferrer-Martinez, A., Ruiz-Lozano, P., and Chien, K.R. (2002). Mouse PeP: a novel peroxisomal protein linked to myoblast differentiation and development. Dev Dyn 224, 154-167.

Jedrychowski, M.P., Wrann, C.D., Paulo, J.A., Gerber, K.K., Szpyt, J., Robinson, M.M., Nair, K.S., Gygi, S.P., and Spiegelman, B.M. (2015). Detection and Quantitation of Circulating Human Irisin by Tandem Mass Spectrometry. Cell Metab 22, 734-740.

Kall, L., Krogh, A., and Sonnhammer, E.L. (2004). A combined transmembrane topology and signal peptide prediction method. J Mol Biol 338, 1027-1036.

Kim, H., Wrann, C.D., Jedrychowski, M., Vidoni, S., Kitase, Y., Nagano, K., Zhou, C., Chou, J., Parkman, V.A., Novick, S.J., et al. (2019). Irisin Mediates Effects on Bone and Fat via alphaV Integrin Receptors. Cell 178, 507-508.

Leal, L.G., Lopes, M.A., and Batista, M.L. (2018) [Review]. Physical Exercise-Induced Myokines and Muscle-Adipose Tissue Crosstalk: A Review of Current Knowledge and the Implications for Health and Metabolic Diseases. Frontiers in Physiology 9.

Li, R.-L., Wu, S.-S., Wu, Y., Wang, X.-X., Chen, H.-Y., Xin, J.-J., Li, H., Lan, J., Xue, K.-Y., Li, X., et al. (2018). Irisin alleviates pressure overload-induced cardiac hypertrophy by inducing protective autophagy via mTOR-independent activation of the AMPK-ULK1 pathway. J Mol Cell Cardiol 121, 242-255.

Lourenco, M.V., Frozza, R.L., de Freitas, G.B., Zhang, H., Kincheski, G.C., Ribeiro, F.C., Gonçalves, R.A., Clarke, J.R., Beckman, D., Staniszewski, A., et al. (2019). Exercise-linked FNDC5/irisin rescues synaptic plasticity and memory defects in Alzheimer's models. Nat Med 25, 165-175.

Michelsen, K., Yuan, H., and Schwappach, B. (2005). Hide and run. Arginine-based endoplasmic-reticulum-sorting motifs in the assembly of heteromultimeric membrane proteins. EMBO Rep 6, 717-722.

Nie, Y. and Liu, D. (2017). N-Glycosylation is required for FDNC5 stabilization and irisin secretion. Biochem J 474, 3167-3177.

Nie, Y.W., Wang, M., Zhang, P., Huan, L., and Liu, D.J. (2016). Identification and characterization of an endoplasmic reticulum localization motif. Biochem Biophys Res Commun 473, 249-254.

Perakakis, N., Triantafyllou, G.A., Fernandez-Real, J.M., Huh, J.Y., Park, K.H., Seufert, J., and Mantzoros, C.S. (2017). Physiology and role of irisin in glucose homeostasis. Nat Rev Endocrinol 13, 324-337.

Petersen, T.N., Brunak, S., von Heijne, G., and Nielsen, H. (2011). SignalP 4.0: discriminating signal peptides from transmembrane regions. Nat Methods 8, 785-786.

Polyzos, S.A., Mathew, H., and Mantzoros, C.S. (2015). Irisin: A true, circulating hormone. Metabolism 64, 1611-1618.

Reza, M.M., Subramaniyam, N., Sim, C.M., Ge, X., Sathiakumar, D., McFarlane, C., Sharma, M., and Kambadur, R. (2017). Irisin is a pro-myogenic factor that induces skeletal muscle hypertrophy and rescues denervation-induced atrophy. Nat Commun 8, 1104.

Sanchis-Gomar, F., Alis, R., and Lippi, G. (2015). Circulating irisin detection: Does it really work? Trends in Endocrinology & Metabolism 26, 335-336.

Teufel, A., Malik, N., Mukhopadhyay, M., and Westphal, H. (2002). Frcp1 and Frcp2, two novel fibronectin type III repeat containing genes. Gene 297, 79-83.

Wrann, C.D., White, J.P., Salogiannnis, J., Laznik-Bogoslavski, D., Wu, J., Ma, D., Lin, J.D., Greenberg, M.E., and Spiegelman, B.M. (2013). Exercise induces hippocampal BDNF through a PGC-1alpha/FNDC5 pathway. Cell Metab 18, 649-659.

Xiong, X.Q., Geng, Z., Zhou, B., Zhang, F., Han, Y., Zhou, Y.B., Wang, J.J., Gao, X.Y., Chen, Q., Li, Y.H., et al. (2018). FNDC5 attenuates adipose tissue inflammation and insulin resistance via AMPK-mediated macrophage polarization in obesity. Metabolism 83, 31-41.

Young, M.F., Valaris, S., and Wrann, C.D. (2019). A role for FNDC5/Irisin in the beneficial effects of exercise on the brain and in neurodegenerative diseases. Progress in Cardiovascular Diseases 62, 172-178.

Zhang, Y., Li, R., Meng, Y., Li, S., Donelan, W., Zhao, Y., Qi, L., Zhang, M., Wang, X., Cui, T., et al. (2014). Irisin stimulates browning of white adipocytes through mitogen-activated protein kinase p38 MAP kinase and ERK MAP kinase signaling. Diabetes 63, 514-525.

Zhou, Q., Chen, K., Liu, P., Gao, Y., Zou, D., Deng, H., Huang, Y., Zhang, Q., Zhu, J., and Mi, M. (2015). Dihydromyricetin stimulates irisin secretion partially via the PGC-1α pathway. Mol Cell Endocrinol 412, 349-357.

Legends

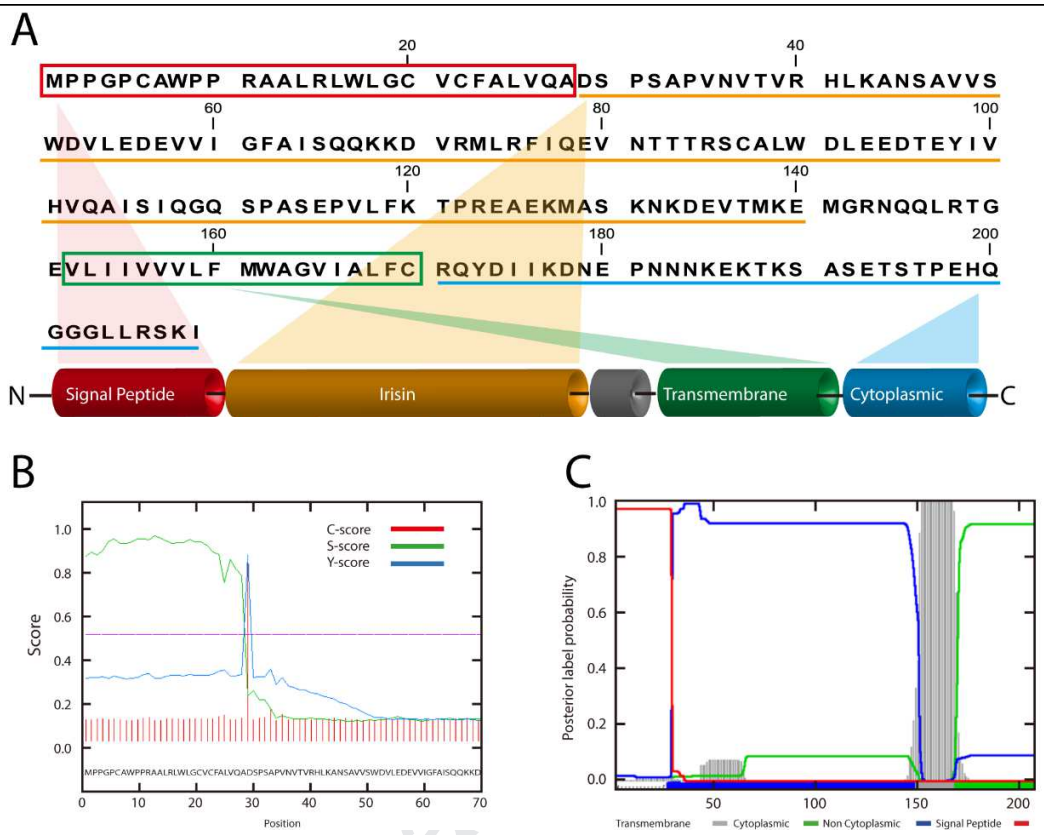

Figure 1. Diagram of the structural domain sequences of FNDC5. (A) Schematic drawing of FNDC5. The signal peptide is boxed in red. The fibronectin type III (FNIII) domain is underlined in yellow. The transmembrane domain is boxed in green. The cytoplasmic domain is underlined in blue. (B) Result of FNDC5 signal peptide analysis using SignalP-software. (C) Result of FNDC5 transmembrane domain analysis using the Phobius web interface.

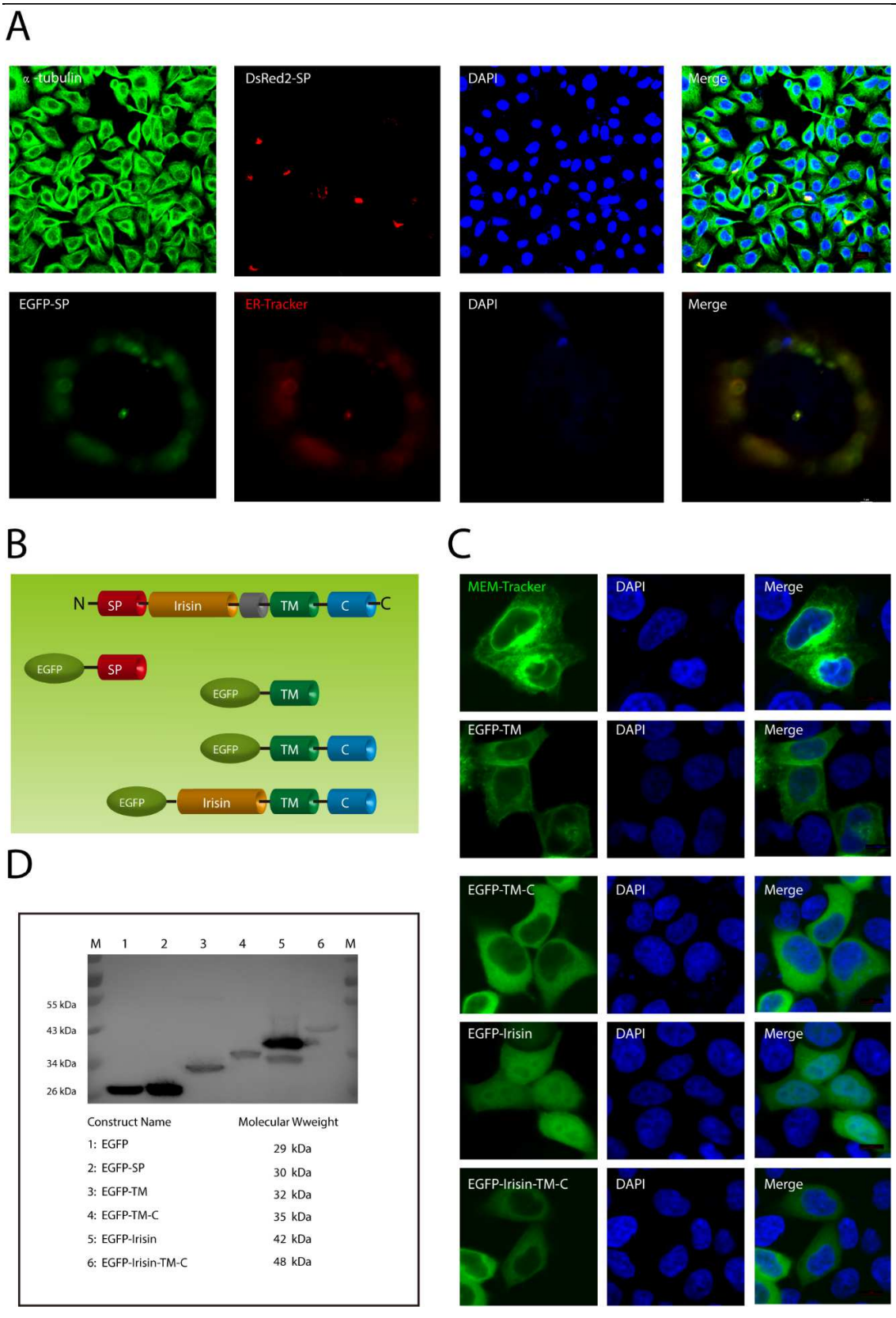
A
α -tubulin
DsRed2-SP
DAPI
Merge
EGFP-SP
ER-Tracker
DAPI
Merge
B
N
SP
Irisin
TM
C
C
EGFP
SP
EGFP
TM
EGFP
TM
C
EGFP
Irisin
TM
C
C
MEM-Tracker
DAPI
Merge
EGFP-TM
DAPI
Merge
EGFP-TM-C
DAPI
Merge
EGFP-Irisin
DAPI
Merge
EGFP-Irisin-TM-C
DAPI
Merge
D
M 1 2 3 4 5 6 M
55 kDa
43 kDa
34 kDa
26 kDa
Construct Name
Molecular Wweight
1: EGFP
29 kDa
2: EGFP-SP
30 kDa
3: EGFP-TM
32 kDa
4: EGFP-TM-C
35 kDa
5: EGFP-Irisin
42 kDa
6: EGFP-Irisin-TM-C
48 kDa

Figure 2. Identification of construct containing transport signal localizations. (A) Representative images of FNDC5 signal peptide intracellular localization. pEGFP-C1-SP and pDsRed2-C1-SP plasmids were transfected into HeLa cells. pDsRed2-ER vector was used as an ER labeling marker (Clontech, USA). α-tubulin was detected using an FITC labeled antibody. Nuclei were stained with DAPI. (B) Schematic representation of the construction of different plasmids. (C) Representative images of intracellular localization of FNDC5 transmembrane domain and construction. pEGFP-C1-TM, pEGFP-C1-TM-C, pEGFP-C1-irisin, and pEGFP-C1-irisin-TM-C plasmids were transfected into HeLa cells. pEYFP-Mem vector (Clontech, USA) was used as aplasma membrane target marker. Nuclei were stained with DAPI. (D) Western blotting analysis was carried out using EGFP antibodies on protein extracts collected from 293T cells transfected with pEGFP-C1 (Lane 1), pEGFP-C1-SP (Lane 2), pEGFP-C1-TM (Lane 3), pEGFP-C1-TM-C (Lane 4), pEGFP-C1-irisin (Lane 5), and pEGFP-C1-irisin-TM-C (Lane 6) plasmids.

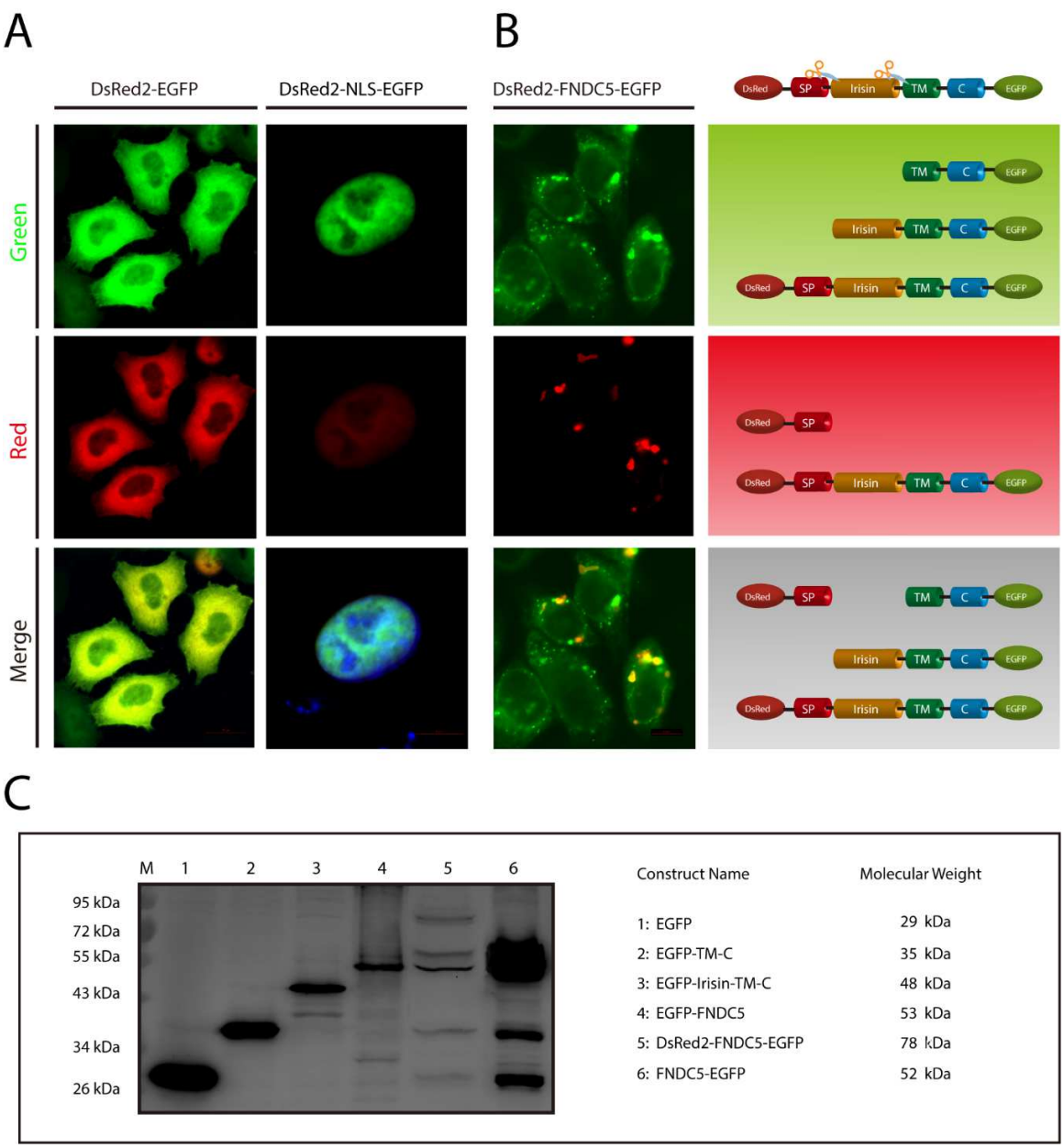

Figure 3. Analysis of FNDC5 cleavage. (A) Representative images of intracellular localization of DsRed2-EGFP and DsRed2-NLS-EGFP proteins. pDsRed2-C1-EGFP-N1 plasmid was used as a non-cleavage cytoplasm localization control. pDsRed2-C1-NLS-EGFP-N1 plasmid was used as a non-cleavage nucleus localization control. Representative images of DsRed2-FNDC5-EGFP protein localization. pDsRed2-C1-FNDC5-EGFP-N1 plasmid was transfected into HeLa cells. (C) Western blotting analysis was carried out using EGFP antibodies on protein extracts collected from 293T cells transfected with pEGFP-C1 (Lane 1), pEGFP-C1-TM-C (Lane 2), pEGFP-C1-irisin-TM-C (Lane 3), pEGFP-C1-FNDC5 (Lane 4), pDsRed2-C1-FNDC5-EGFP-N1 (Lane 5), and pEGFP-N1-FNDC5 (Lane 6) plasmids.

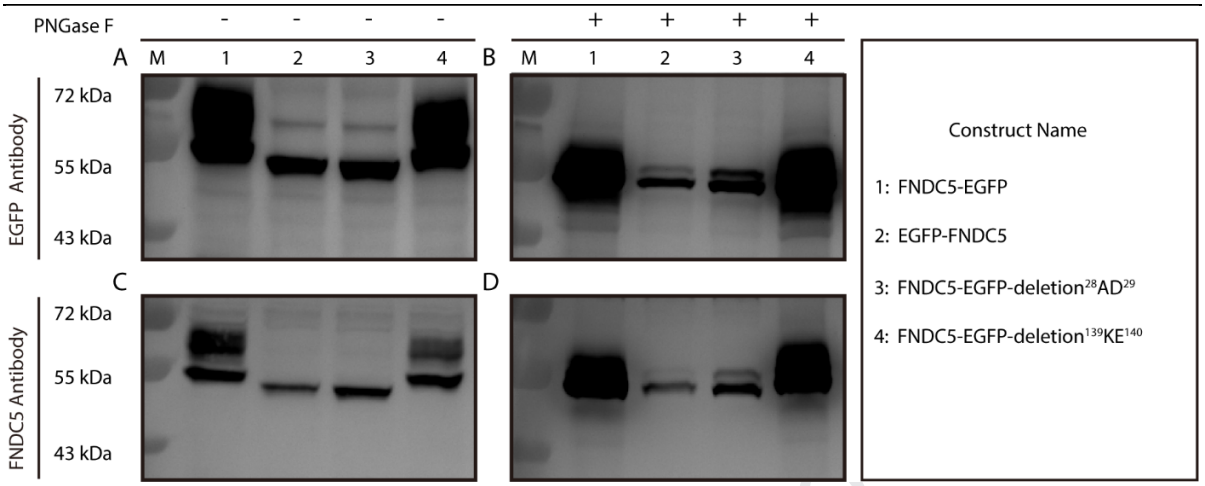

Figure 4. Effect of mutation on FNDC5 N-glycosylation. 293T cells were transfected with pEGFP-N1-FNDC5 (Lane 1), pEGFP-C1-FNDC5 (Lane 2), pEGFP-N1-FNDC5-deletion^{28}AD^{29} (Lane 3), and pEGFP-N1-FNDC5-deletion^{139}KE^{140} (Lane 4) plasmids. Protein lysates (20 μg protein per lane) were immunoblotted after treatment (+) or non-treatment (−) with PNGase F. Western blotting analysis was carried out using EGFP and FNDC5 antibodies.

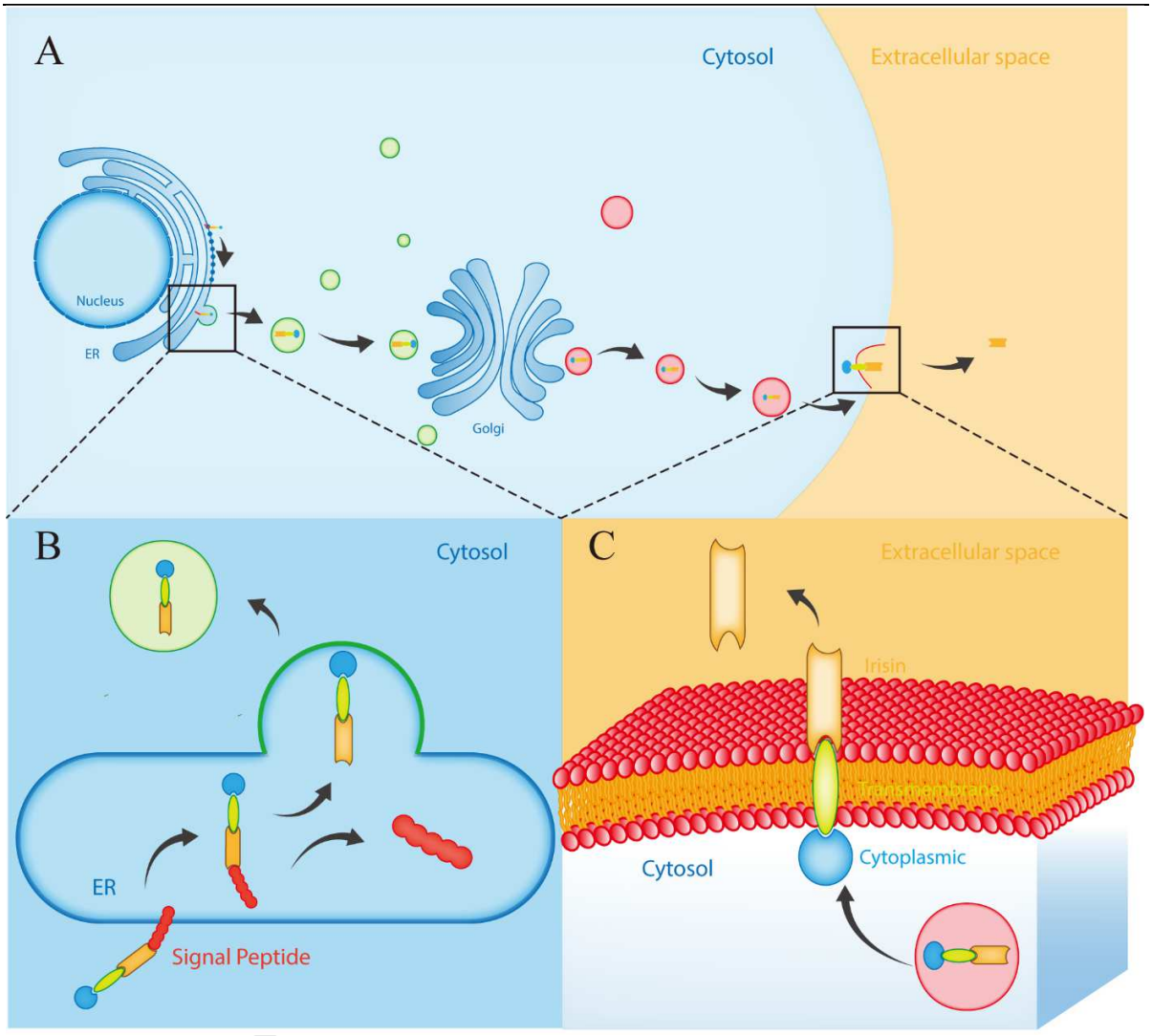

Figure 5. Model of FNDC5 maturation and cleavage. Nascent FNDC5 proteins are translated in the ER. Once the FNDC5 protein is ready for forward traffic, signal peptide sequence cleavage activity operates to ensure that FNDC5 is not recognized by the retrieval or retention machinery before the N-glycosylated FNDC5 is fully folded and assembled. Ectodomain cleavage occurs on the cell plasma membrane. Subsequent to ectodomain cleavage, irisin is generated. The ectodomain cleavage of FNDC5 must be tightly regulated, as the permanent release of irisin is incompatible with a state of health. In addition, it is an area lacking information regarding the precise ectodomain cleavage site, and furthermore, the molecular mechanism of FNDC5 cleavage regulation.

Highlights

- The signal peptide responsible for ER targeting of FNDC5 was identified
- FNDC5 ectodomain was cleaved from its signal peptide and transmembrane attachment
- Genetic ablation of the signal peptide cleavage site blocked FNDC5 N-glycosylation